

## **General Disclaimer**

### **One or more of the Following Statements may affect this Document**

- This document has been reproduced from the best copy furnished by the organizational source. It is being released in the interest of making available as much information as possible.
- This document may contain data, which exceeds the sheet parameters. It was furnished in this condition by the organizational source and is the best copy available.
- This document may contain tone-on-tone or color graphs, charts and/or pictures, which have been reproduced in black and white.
- This document is paginated as submitted by the original source.
- Portions of this document are not fully legible due to the historical nature of some of the material. However, it is the best reproduction available from the original submission.

311

*No*

MSC INTERNAL NOTE NO. 66-EG-13

PROJECT APOLLO

A SIMULATION STUDY OF MANUAL CONTROL TECHNIQUES FOR THE  
CONCENTRIC FLIGHT PLAN OF LUNAR ORBIT RENDEZVOUS

Prepared by: Ronald W. Simpson  
Ronald W. Simpson

Approved by: David W. Gilbert  
David W. Gilbert, Chief,  
Engineering Simulation Branch

Approved by: Robert G. Chilton  
Robert G. Chilton, Deputy Chief,  
Guidance and Control Division

NATIONAL AERONAUTICS AND SPACE ADMINISTRATION

MANNED SPACECRAFT CENTER

Houston, Texas

March 18, 1966



FACILITY FORM 602

N70 247 60 (THRU)  
39 (PAGES)  
TMX 64308 (NASA CR OR TMX OR AD NUMBER)  
21 (CATEGORY)

## INTRODUCTION

To insure a high probability of success of the LEM/CSM lunar orbit rendezvous, procedures must be developed for monitoring of the primary G&N system, monitoring of the transfer orbit, and providing for backup navigation and control in the event of a partial or complete primary G&N system failure. Some progress has already been made toward establishing these procedures. Studies have been conducted by the NASA and at contractor facilities (references 1 to 4) relative to both Gemini/Agona rendezvous maneuvers and to LEM/CSM lunar orbit rendezvous in which monitoring and backup control requirements have been investigated. All of these studies have been useful in providing information that can be either extrapolated or applied directly to the lunar rendezvous maneuver.

More recently, the Guidance and Control Division conducted a simulation study of the lunar orbit rendezvous to evaluate control modes which could possibly backup the primary guidance system (reference 5). This particular study assumed a direct-ascent flight plan for LEM/CSM rendezvous and the existence of an on-board rendezvous radar in the LEM. The present study, described herein, is based on a parking orbit mode of rendezvous termed the concentric flight plan (CFP). It could be implemented with either a rendezvous radar (RR) or a LEM optical rendezvous system (LORS). The purpose of this simulation was to (1) determine the best braking schedule for the CFP, (2) evaluate possible backup control modes for the CFP assuming an optical tracker, and (3) compare the  $\Delta V$  performance of backup control modes for the LEM using the optical tracker with that of the LEM using the rendezvous radar.

## SCOPE OF STUDY

For this study it was assumed that the primary system had failed prior to the transfer injection maneuver and that the transfer injection and midcourse correction maneuvers had been made with the AGS using MSFN navigation data.

The backup control modes were evaluated for the terminal phase of rendezvous. Each transfer was initiated at an approximate range of 60,000 feet and terminated at a range of the order of 100 feet with a range-rate of less than 1 fps. An illustration of the nominal CFP and the portion studied in this simulation is given in figure 1. The basic assumptions used in this study were (1) the CSM could be seen from the LEM by the unaided eye at a range of 15 n.m. because of the luminous beacon on the CSM or sunlight reflected off the CSM; (2) sufficient ground tracking was available to allow MSFN to update the LEM with relative range to CSM, relative range-rate, and transfer altitude prior to the terminal phase; and (3) the LEM spacecraft was attitude stabilized using the abort guidance section (AGS) inertial reference system.

## SYMBOLS

$(A, E)$	Azimuth and elevation angles of the CSM with respect to the LEM body axis system, degrees
$[B]$	Euler angle transformation matrix from inertial to LEM body axis system
$[B]^{-1}$	Inverse of $[B]$ .
$(F_x, F_y, F_z)$	Body translation thrusts transformed to the inertial axes, lb
$g$	Earth gravity, $32.2 \text{ ft/sec}^2$
$G$	Universal gravitation potential, $3.44 \times 10^{-8} \text{ ft}^4/\text{lb-sec}^4$
$I_{sp}(\text{RCS})$	Specific impulse of RCS jet fuel, sec
$I_{sp}(\text{ASC})$	Specific impulse of ascent engine fuel, sec
$(I_{xx}, I_{yy}, I_{zz})$	Moments of inertia of LEM about its principal axes, slug-ft <sup>2</sup>
$(I_{xy}, I_{xz}, I_{yz})$	Products of inertia of LEM, slug-ft <sup>2</sup>
$K_A$	Attitude feedback gain
$K_R$	Rate feedback gain
$K_S$	Attitude controller gain
$(l_q, l_r, l_p)$	Attitude control moment arms, ft
$l_z$	Characteristic jet damping moment arm, $ z_{cg} - z_{ASCXP} $ , ft
$m$	Mass of LEM, slugs
$M$	Mass of moon, $5.02085 \times 10^{21}$ slugs
$(M_{cq}, M_{cr}, M_{cp})$	Attitude control moments of LEM, ft-lb
$(q, r, p)$	LEM angular rates about its body axes, deg/sec
$\bar{r}_f$	Inertial position vector of LEM, ft
$(r_{fx}, r_{fy}, r_{fz})$	Components of $\bar{r}_f$ , ft.

SYMBOLS (Continued)

$\bar{r}_s$	Inertial position vector of CSM, ft
$\bar{R}$	Range vector of LEM with respect to CSM, ft
$S$	Laplace operator
$(T_{1\dots 16})$	LEM RCS thrusters
$T_{ASC}$	Ascent engine thrust, lb
$T_{RCS}$	RCS thrust, lb
$(T_x, T_y, T_z)$	Total thrust along the LEM $X_b, Y_b, Z_b$ axes, lb
$\Delta V$	Characteristic velocity, ft/sec
$X_{cg}$	Location of LEM c.g. along the $X_b$ axis, ft
$(X_b, Y_b, Z_b)$	LEM body axes
$(X_B, Y_B, Z_B)$	Components of $\bar{R}$ along the LEM body axes, ft
$(X_I, Y_I, Z_I)$	Components of $\bar{R}$ along the inertial axes, ft
$\bar{Y}_{cg}$	Location of LEM cg along the $Y_b$ axis, ft
$\bar{Z}_{cg}$	Location of LEM cg along the $Z_b$ axis, ft
$Z_{pads}$	Location of LEM leg pads along the $Z_b$ axis, ft
$Z_{RCS}$	Location of LEM RCS jet plane along the $Z_b$ axis, ft
$Z_{ASC}$	Location of LEM ascent engine attachment point, ft
$Z_{ASCXP}$	Location of LEM ascent engine exit plane, ft
$\epsilon$	Error signal
$(\epsilon_\theta, \epsilon_\psi, \epsilon_\phi)$	Pitch, yaw, and roll error signals
$(\epsilon_{\theta_B}, \epsilon_{\psi_B}, \epsilon_{\phi_B})$	Pitch, yaw, and roll error signals transformed to the LEM body axes
$(\theta, \psi, \phi)$	Pitch, yaw, and roll angles, degrees

$(\theta_c, \psi_c, \phi_c)$	Pitch, yaw, and roll commanded angles, degrees
$\lambda$	Central angle to CSM measured from landing site, degrees
$\tau_1$	Time delay of RCS jets, sec
$\tau_2$	Time delay of reference attitude feedback signal, sec
$\omega$	Angular velocity of the CSM local vertical, rad/sec

#### SUBSCRIPTS

o	Initial value
t	With respect to time

One dot over a quantity denotes the first derivative with respect to time and two dots over a quantity denotes the second derivative with respect to time. An arrow over a quantity denotes a vector.

## DESCRIPTION OF SIMULATION

## General

The LEM and CSM were simulated in six and three-degrees-of-freedom, respectively, using general purpose computing equipment coupled with a fixed-base simulator cockpit containing the pilot controls and instrument displays and an out-the-window display. A block diagram of the computer mechanization is shown in figure 2. The translation equations of motion of the LEM relative to the CSM were mechanized on a digital differential analyzer (DDA). A general purpose digital computer was utilized for inputs to and outputs from the problem and for controlling the operational modes of the DDA. The rotational equations of motion of the LEM relative to an inertial set of axes were mechanized on an analog computer. Another analog computer was used to continuously compute inertial-to-body and body-to-inertial transformations, which in turn, were used to compute target line-of-sight information. The analog computers received inertial position and velocity data from the DDA through digital to analog converters. The jet select logic was mechanized using special purpose electronics.

A virtual image optical display system was used to present an out-the-window display of the CSM to the pilot. For the purposes of this study, the CSM was represented by small light source in the display until a relative range of 1500 feet was reached. At this range, target growth became apparent and continued to increase until it appeared as a 16-foot square planar surface at zero range. Inertial velocity data were fed to the special purpose digital display computer to continuously update the target position. Control of the terminal rendezvous was maintained by the pilot through monitoring of the flight instruments and visual displays.

## Equations of Motion

The relative motion of the LEM with respect to the CSM was expressed in six-degrees-of-freedom and was represented by translation and rotation equations of motion which were derived for an inertial coordinate system centered in the moon as shown in figure 1. The moon model was considered to be spherical and nonrotational. The  $Z_I$ -axis is directed positive away from the landing site (landing site vertical), the  $X_I$ -axis is parallel to the landing site horizontal pointing west, and the  $Y_I$ -axis completes the right-handed set. A detailed block diagram of the translation equations of motion are shown in figure 3.

The rotation equations of motion, as mechanized in the attitude control system, for the pitch, yaw, and roll axes are shown in figures 4, 5, and 6, respectively. The body axes are defined for the LEM in figure 7 and the Euler angle sequence used to reference the LEM body axes with respect to the inertial reference was  $\theta$ ,  $\psi$ ,  $\phi$ .

#### Simulated LEM

The LEM mass was given an initial value of 159 slugs and changed as attitude and translation fuel was consumed. An Isp of 275 seconds was used for the RCS jets. Ascent engine thrust was not used. Details of the moments and products of inertia used in the simulation are given in Appendix A.

Cockpit Displays.- LEM flight displays used in the study were: range, range-rate, attitude and attitude rate, LOS angles, LOS angular rates,  $\Delta V$ , percent fuel remaining, and event timer. An MK9 gunsight was used as a collimated reticle and was boresighted along the X-axis. A 5-digit DVM was used to simulate the data entry and display assembly (DEDA) of the abort guidance section (AGS). A photograph of the controls and displays of the simulated LEM cockpit is given in figure 8.

Translational Control.- Translation control was obtained using only the RCS jets. Signals from the LEM translation control stick were applied to a jet select logic box. On-off thruster firing with a thrust buildup and delay time constant of 15 milliseconds was used to simulate the actual reaction jet response. Translation acceleration was  $1.25 \text{ fps}^2$  using two jets. A two-position switch allowed four jets to be used when desired, which gave an acceleration of  $2.5 \text{ fps}^2$  in the direction of the minus Z-body axis.

Attitude Control.- Since the primary system was assumed to have failed, the attitude control modes simulated were those normally available with the LEM SCS, i.e., (1) NORMAL (PRM-rate command attitude hold), (2) PULSE (minimum impulse-open loop), and (3) DIRECT (on-off-open loop). These modes of operation were implemented by directing signals from an Apollo attitude controller to the jet select logic and signal modulation box. The attitude control accelerations for pilot pitch, roll, and yaw were 24.7, 42.7, and 21.0 degrees per second per second, respectively, using two RCS jets. The maximum attitude rate was limited to 20 degrees per second in NORMAL mode.

Abort Guidance Section.- Two possible configurations were simulated. Both assumed that the AGS could perform the rendezvous transfer injection and could make midcourse corrections using an external navigation source. However, in the first configuration it was assumed that the AGS did not have the capability to compute range and range-rate for pilot display. In this configuration, a continuous estimation of range and range-rate was obtained by the pilot using elapsed time, as displayed on the DEDA, and flight charts. The second configuration assumed that the AGS could continuously compute range and range-rate for pilot display. These two quantities could be selected on the DEDA using a two-position toggle switch.

Rendezvous Radar.- The simulated LEM RR presented displays of range, range-rate, LOS angles, and LOS rates. These radar quantities were displayed to the pilot only for the backup control mode which assumed the RR as the LEM on-board navigation source. The current error model of the LEM RR was used, the most significant error being a 0.2 mr/sec uncertainty in the LOS rate.

#### Data Acquisition

Data were obtained for each run by a digital printout of pertinent variables every 60 seconds. The variables recorded were: (1) components of relative position vector of LEM ( $X, Y, Z$ ), (2) components of relative velocity vector of LEM ( $\dot{X}, \dot{Y}, \dot{Z}$ ), (3) range ( $R$ ), (4) range-rate ( $\dot{R}$ ), (5) azimuth rate ( $\dot{A}$ ), (6) elevation rate ( $\dot{E}$ ), (7) relative velocity change due to thrust ( $\Delta V$ ), (8) elapsed time ( $t$ ), (9) attitude fuel used ( $W_A$ ), and (10) translation fuel used ( $W_T$ ). In addition, two variplotters were used to obtain histories of  $R$  versus  $R$  and  $X$  versus  $Z$  for each run.

#### CFP TRANSFER ORBITS STUDIED

Three different transfer orbits associated with the concentric flight plan were used as a basis for the study. They are as follows:

1. 140-degree transfer from 65 n.m. circular orbit to 80 n.m. circular orbit (nominal launch-intercept velocity of 29 fps\*)
2. 140-degree transfer from 30 n.m. circular orbit to 80 n.m. circular orbit (late launch-intercept velocity of 74 fps\*)
3. 140-degree transfer from 118 n.m. circular orbit to 80 n.m. circular orbit (abort from powered descent-intercept velocity of 54 fps\*)

\*The value of  $\mu$  used in the simulation  $1.729344 \times 10^{14}$ .

Figure 9 illustrates the relative path flown by LEM for the transfers cited above. The transfer paths are referenced to the CSM local vertical reference frame. The initial conditions for the above three intercept transfers are given in Appendix B.

#### Initial Condition Errors

For this study, it was assumed that the primary system had failed prior to the transfer injection maneuver and that the transfer injection and midcourse correction maneuvers had been made with the AGS using MSFN navigation data. Thus, it was possible for certain position and velocity errors to exist at the beginning of the terminal phase.

To simulate the MSFN navigation errors involved, random component initial condition errors were generated using the MSFN error covariance matrix obtained from MPAD. (These errors are comparable to MSFN performance given in MPAD memo No. 66-FM4-58.) The following standard deviations were obtained from this matrix:

$\sigma_{\text{range}} = 333$ feet	
$\sigma_{\text{range-rate}} = 0.320$ fps	
$\sigma_{\text{in-plane LOS}} = 170$ feet	} perpendicular to range vector
$\sigma_{\text{in-plane LOS rate}} = 0.16$ fps	
$\sigma_{\text{out-of-plane LOS}} = 813$ feet	} perpendicular to range vector
$\sigma_{\text{out-of-plane LOS rate}} = 0.75$ fps	

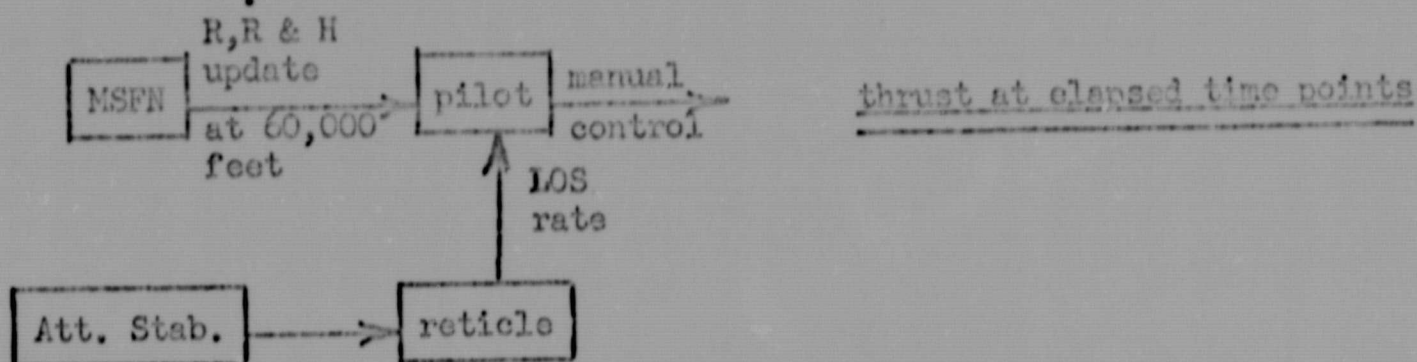
To be certain that the backup control modes would be evaluated for worst case MSFN performance, random component error vectors were generated which were approximately 4.5 times as large as those given above.

#### BACKUP CONTROL MODES INVESTIGATED

The following PNGS-AGS configurations were investigated:

Case 1.-- The primary navigation sensor for the LEM was LORS; however, it was assumed that MSFN was the only remaining navigation source for state vector updates. This assumes a failure in LORS or LGC plus a CSM-AGC, CSM-SXT, or SCM-VHF failure. For this case, the AGS did not have the capability to compute and display range and range-rate to the pilot for

terminal control. A block diagram of the backup control mode simulated is given below:



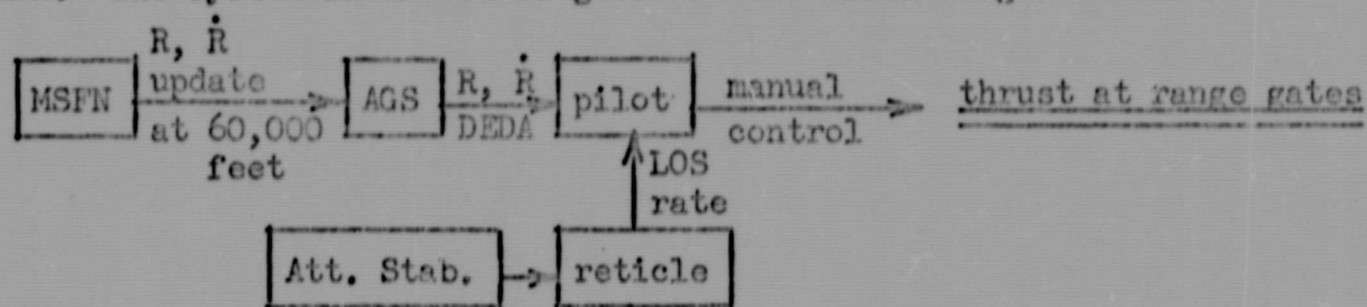
The control procedures used with this backup control mode are as follows:

LOS-Rate Control - The procedures given below are used to monitor and control the LOS-rate continuously except during range-rate braking maneuvers.

Procedure No.	Task
1.	Center target in reticle using spacecraft attitude control; put spacecraft in attitude-hold control mode.
2.	Determine elapsed time (using event timer) required for target to drift to 50 mr circle of reticle.
3.	If the elapsed time was greater than 250 seconds go back to procedure no. 1; if elapsed time was less than 250 seconds, to to procedure No. 4.
4.	Determine LOS-rate magnitude using figure 13.
5.	Determine correction required in LOS-rate magnitude using figure 14 (use of this chart is explained in DISCUSSION OF BACKUP TECHNIQUES).
6.	Roll spacecraft (pilot roll) so that LOS motion is parallel to spacecraft vertical or lateral axis.
7.	Center target in reticle using spacecraft attitude control.
8.	Make required LOS-rate correction using spacecraft translation control ( $\Delta V$ is monitored using AGS $\Delta V$ indication).
9.	Go to procedure No. 1.

Range-Rate Control.- Make range-rate braking maneuvers at elapsed time points indicated in figure 10 (use of this chart is explained in DISCUSSION OF BACKUP TECHNIQUES).

Case 2.- The configuration of this backup mode was the same as for case 1 except that it was assumed the AGS had the capability to integrate the trajectory thereby providing a display of range and range-rate on the DEDA. The system simulated is given in the block diagram below:



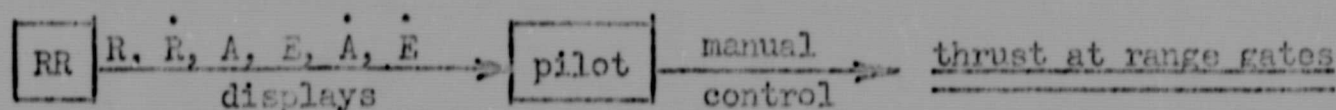
The control procedures used with this backup control mode are as follows:

LOS-Rate Control.- The procedures given below are used to monitor LOS-rate continuously and make corrections at range gates.\*

Procedure No.	Task
1.	Center target in reticle using spacecraft attitude control; put spacecraft in attitude-hold control mode.
2.	Determine elapsed time (using event timer) for target to drift to 50 mr circle of reticle.
3.	Make LOS-rate corrections as required (i.e., when timed LOS-rate is above 0.2 mr/sec) at each range gate given in figure 15. This chart gives the thrust direction (referenced to LOS) required for a combined LOS-rate and range-rate correction at each range gate. Details of the use of this chart are given in DISCUSSION OF BACKUP TECHNIQUES.
	*Make LOS-rate corrections between range gates <u>only</u> when it appears that the range-rate will drop below the range-rate specified for the next range gate before that range gate is reached.

Range-Rate Control.- Make range-rate braking maneuvers as required at each range gate given in figure 15.

Case 3.- This backup control mode assumed that the LEM contained a RR. It was also assumed that the LGC had failed so that the RR displays were used directly by the pilot for manual control of the terminal phase of rendezvous. The block diagram of this system is shown below:



LOS-rate and range-rate corrections are made at range gates using a chart similar to that of figure 15. Deviations from this chart are explained in DISCUSSION OF BACKUP TECHNIQUES.

#### TEST SUBJECTS

Three test subjects flew a major portion of the simulator runs: an engineer-pilot with 2500 hours aircraft flying time and 1200 hours simulator time, an engineer with approximately 1000 hours simulator time flying LEM and Gemini rendezvous but no aircraft flying experience, and an engineer with 10 hours simulator prior to this study. After the test matrix was complete, five astronauts made several familiarization runs each.

#### TEST MATRIX

The test matrix used in the simulation is given in appendix C. Runs were made for the CFP transfers discussed earlier using 1, 2, and  $4.5\sigma$  MSFN errors generated randomly.

In addition to these test cases, several runs were made using the case 1 backup control mode for a critical failure. First, it was assumed that the PNGS obtained a navigation update using LORS just prior to the ascent maneuver. Then it was assumed that no navigation update was available to the LEM after ascent injection. Thus, the LEM PNGS operated open loop for the remaining thrust maneuvers of the CFP and the ascent errors were propagated to the beginning of the terminal phase of rendezvous. This error propagation resulted in standard deviations for range and range-rate of 10,000 feet and 16 fps, respectively. These propagated errors were used to generate random initial condition errors for the 30 n.mi. to 80 n.mi. transfer.

## DISCUSSION OF BACKUP TECHNIQUES

## MSFN -- No AGS computations (Case 1)

For case 1, it was assumed MSFN gave the LEM pilot an update of range, range-rate, and transfer altitude at the beginning of the terminal phase. From this point on, the pilot continuously obtained current estimates of range and range-rate using elapsed time from the start of the problem and the range/range-rate time history chart shown in figure 10. This technique is based on the fact that if adequate line-of-sight rate control is maintained, the range and range-rate for an intercept transfer can be prepared beforehand in chart form as function of elapsed time from a set of initial conditions for different transfer altitudes. Figure 10 is such a chart. Thus, the first range-rate braking maneuver was made when the elapsed time reached that indicated by the intersection of the dashed line shown on the chart and the range/range-rate time history corresponding to the particular transfer being flown. At this point, the range-rate was reduced to 25 fps using the  $\Delta V$  indication of the AGS. The next braking maneuver came after the pilot determined an apparent target growth which was programmed to begin at a relative LEM-CSM range of 1500 feet. Thus, the second braking maneuver usually occurred at a range of the order of 900 feet. The range-rate was reduced to 5 fps, again using the AGS  $\Delta V$  indication. The final 5 fps of range-rate was cancelled when an estimated range of 100 feet or less was reached.

To determine what LOS-rates were required for efficient transfers, time histories of LOS-rate versus range were studied for the different CFP transfers. These time histories are shown in figure 11. It can be seen that the LOS-rate approaches zero as range approaches zero for all the transfers given (only true for intercept transfers). Also, it can be seen that the outer limits of all the LOS-rate plots can be represented by the dashed lines as shown. Satisfactory LOS-rate control could be maintained by keeping the LOS-rate within the area bounded by these dashed lines. These limits would be used as shown if it were possible to determine the LOS-rate exactly. However, because of sensor errors, the control limits must be modified, depending upon the magnitude of uncertainty in LOS-rate. For the backup control mode under discussion, the LOS-rate was determined with the use of a MK9 gunsight used as a collimated reticle. By making sightings with this reticle and comparing the LOS-rate obtained with the true LOS-rate given by the simulation computer, it was found that the LOS-rate uncertainty was usually below 0.1 mr/sec. Thus, the upper limit on LOS rate was maintained at 0.2 mr/sec from 45,000 feet to 0 feet range.

To monitor and control the LOS-rate down to the 0.2 mr/sec limit, the pilot continuously timed the LOS-rate with a reticle pattern as shown in figure 12. Because the limit cycle motion was simulated, the pilot had to estimate when the center of the limit cycle was coincident with the intersection of the cross hairs (the deadband of  $\pm 0.3$  degrees is approximately equivalent to  $\pm 10$  mr). The pilot then recorded the time

required for the target to drift to the first circle (50 mr radius). Again, the pilot had to estimate when the center of the limit cycle fell on the circle being used (for high LOS rates, the 100 mr radius circle was used). The chart shown in figure 13 was then used to determine the LOS rate in mr/sec. Finally, the pilot used the chart shown in figure 14 to determine the LOS rate correction in fps if one was required (that is, if the timed LOS rate was above 0.2 mr/sec). The pilot used the chart in the following manner:

1. find intersection of timed LOS rate with range corresponding to current range estimation (range estimated using elapsed time from start of problem and chart shown in figure 10);
2. record LOS rate in fps for this intersection point;
3. follow constant range line down to intersection with dashed line;
4. record LOS rate in fps for this intersection point;
5. difference between the two LOS rates is the correction required. The pilot then made the correction in the direction of target drift.

When simulator runs were made using the 30 to 80 n.m. transfer where ascent errors had been propagated to the beginning of the terminal phase, this backup control mode was also used. However, one significant change was made in the backup mode configuration. No MSFN update was given to the pilot at the beginning of the terminal phase. Thus, the only information the pilot had concerning his range and range-rate were the nominal values given in the chart of figure 10 and the knowledge that errors in range and range-rate were defined by  $\sigma$  range = 10,000 feet and  $\sigma$  range-rate = 16 fps. In this case, figure 10 would have to cover the elapsed time from the transfer maneuver. Because of these large uncertainties, the first range-rate braking maneuver was made at an estimated range of 18,000 feet rather than 10,000 feet. Also, the range-rate was only reduced down to an estimated -63 fps instead of -25 fps. This assured an intercept velocity of at least -25 fps in the event the errors in range-rate were  $3\sigma$  on the low side. The LOS rates were controlled in the manner indicated above.

#### MSFN-AGS Computations (Case 2)

The configuration used in this case was identical to case 1 except that the AGS was assumed to be able to integrate the trajectory and provide range and range-rate through the DEDA. Because it was possible to display either of these two quantities at any time, the range-rate braking maneuvers were made at range gates rather than elapsed time intervals. The chart shown in figure 15 was used to combine the LOS-rate

and range-rate corrections into one burn. The manner in which this chart was used is as follows:

1. After the current LOS-rate and range-rate have been determined, locate the intersection of these two quantities for the upcoming range gate. This intersection determines the correct LOS angle to be used for the upcoming thrust maneuver. An intersection above the  $45^\circ$  line indicates that the vertical jets should be used if the LOS-rate is parallel to this axis or the lateral jets if the LOS-rate is parallel to the lateral spacecraft axis. For intersections below the  $45^\circ$  line, the longitudinal jets are always used. This allows the LOS angle to always be maintained below  $45^\circ$ .

2. Control the attitude of the spacecraft to the required azimuth or elevation angle.

3. Thrust in the required direction until the LOS-rate and range-rate have been reduced to the lowest value given on the scales for the current range gate.

However, LOS-rate corrections were also made between range gates when it appeared to the pilot that the range-rate would drop below the range-rate specified for the next range gate. A collimated reticle was again used for LOS-rate determination and the rate was reduced to 0.2 mr/sec at each range gate as shown in the chart. It should be noted that although the chart gives range gates all the way from 120,000 feet range, the first two range gates do not apply to the CFP. All nine range range gates, however, are used for direct ascent transfers. The last range gate is for a range of 100 feet. At any range gate, the range-rate is controlled to that value indicated at the left end of the range-rate scale for that particular range gate. Seven range gates are used for the case 2 backup mode compared to three range gates for case 1 because of the difference in determining range and range-rate. If the type of braking schedule used for case 2 backup mode were used for case 1 backup mode, then for some transfers, a braking maneuver would be made as far out as 60,000 feet range. If this were done, then the range/range-rate time history chart (figure 10) could no longer be used for the remainder of the transfer. Since, for the case 1 backup mode, the first range-rate braking maneuver is delayed until an estimated range of 10,000 feet is reached, the pilot can use the chart all the way into the point where target growth becomes apparent. Delaying the first braking maneuver until 10,000 feet range also assures the pilot that the closure rate is high enough to insure an intercept even if the LOS-rate control is not precise. In case 2, the abort sensor assembly (ASA) senses any braking maneuvers made, and thus, the AGS is able to provide current range and range-rate no matter where the braking maneuvers are made. Because of this, the braking maneuvers can be spread over a greater range to allow for a more comfortable braking schedule.

### Rendezvous Radar (Case 3)

This backup mode required a chart similar to the one shown in figure 15 for vector summing of the R and LOS-rate corrections. The only difference in the chart used for this backup mode from the one used for case 2 was that the LOS-rate was controlled down to 0.3 mr/sec for all range gates from 60,000 feet instead of 0.2 mr/sec for all range gates from 45,000 feet. The reason for this is that the LOS-rate uncertainty using radar is  $\pm 0.2$  mr/sec which is 0.1 mr/sec higher than the uncertainty using a reticle.

### DISCUSSION OF TEST RESULTS

#### Range-Rate Braking Schedule for CFP

Prior to this study, it was known that the most economical range-rate braking schedule for any rendezvous transfer was one which does not increase the range-rate unnecessarily at any of the range gates. However, other factors must also be considered. First, the  $\Delta V$  required at any range gate is limited by the acceleration capability of the spacecraft and the allowable thrust duration of the engines. Secondly, the total  $\Delta V$  required for the terminal maneuver should be divided approximately equally between all the range gates used to allow time to monitor the LOS-rate between each range gate.

For the CFP, it was found that a very good braking schedule could be obtained simply by constraining the range gates and associated range-rates to fall on the range/range-rate time history plot for the nominal CFP transfer (65 n.m. - 80 n.m.). The reason for using this transfer was that, of all the transfers possible which circularize between the altitudes of 30 n.m. and 65 n.m., this one has the lowest intercept velocity. Results indicate that the same braking schedule will be equally economical for all the other transfers because the range-rate will not be increased at any range gate. Of course, as the closer ranges are approached, the range/range-rate gates deviate from the range/range-rate time history of the 65 n.m. - 80 n.m. transfer so that the intercept velocity will be 0 fps instead of 29 fps. The range rate braking schedule which evolved from this study (for manual control) is given below:

## Range-Rate Braking Schedule\*

Range (feet)	Range-Rate (fps)
120,000**	130**
90,000**	100**
-----	
60,000	70
45,000	60
30,000	50
15,000	35
5,000	15
1,000	5
100	1

\*It should be noted that a  $\mu$  of  $1.729344 \times 10^{14}$  was used in determining this braking schedule. The current value of  $\mu$  for the moon (officially documented by NASA) is  $1.73 \times 10^{14}$  and thus, the above braking schedule should be slightly modified for actual LEM flights:

\*\*Used only for direct ascent.

 $\Delta V$  Performance of Backup Control Modes

Effect of MSFN Errors.- A summary of the  $\Delta V$  performance obtained for the three backup control modes investigated is given in figure 16. The bar charts indicate the average  $\Delta V$  used by each backup control mode for each of the three transfers flown. The averages and standard deviations shown were calculated only for the runs made with 1 and 2  $\sigma$  MSFN navigation errors. Individual data points are plotted for the runs made with 4.5  $\sigma$  MSFN navigation errors.

For the 65 to 80 n.m. transfer and 30 to 80 n.m. transfer, the chart shows that the  $\Delta V$  averages and standard deviations are very nearly equal for all three backup modes evaluated. On the 118 to 80 n.m. transfer, the RR backup mode used, on the average, 11 fps less  $\Delta V$  than the backup mode where only MSFN data were used with charts and a reticle. This, however, is not a significant saving by itself as it amounts to about 5 pounds of fuel. With the exception of three of the 18 data points, the cases using 4.5  $\sigma$  MSFN errors required 3 to 13 fps more  $\Delta V$  than the average for the 1  $\sigma$  cases. For the 65 to 80 n.m. transfer using 4.5  $\sigma$  errors, one of the runs made with MSFN/AGS required a  $\Delta V$  of 66 fps which was 26 fps over the average. In examining the data obtained, it was determined that two bad LOS-rate corrections were made on this run which accounts for the increase in  $\Delta V$ . The other two runs not agreeing with the rest of the data were runs made with RR for the 30 to 80 n.m. transfer using 4.5  $\sigma$  errors. The  $\Delta V$  used in both of these runs was below the  $\Delta V$  average for RR and 1  $\sigma$  MSFN errors. After examining the data for these runs, no discrepancy could be found. Thus, it appears that the pilot merely made two very good runs in succession.

Effect of Propagated Ascent Errors.- Five runs were made for the 30 to 80 n.m. transfer where ascent errors were propagated to the beginning of the terminal phase. As stated earlier, these errors resulted in standard deviations in range and range-rate of 10,000 feet and 16 fps, respectively. The average  $\Delta V$  used for these runs is also indicated in figure 16. As shown, the average  $\Delta V$  was 128 fps with a standard deviation of 13 fps. This is an increase of 34 fps over the average  $\Delta V$  used where MSFN navigation was used for midcourse corrections and pilot updating. This increase was caused by two factors: (1) large uncertainties in range and range-rate (pilot allowed for 3  $\sigma$  errors in range and range-rate) and (2) actual errors in range and range-rate. For this particular transfer (30 n.m. to 80 n.m.), the intercept velocity is 74 fps. To insure an intercept velocity of 25 fps with the trajectory errors that were possible, the range-rate had to be controlled in such a manner that caused the range-rate to be high for the transfers flown with zero errors or with errors which increased rather than decreased the range-rate. Because of this, the CSM was passed up in three of the five runs made. In these three runs, the target was passed up 500 feet, 1000 feet, and 3500 feet; however, the pilot had no control problem in getting back to the target other than using slightly more fuel than usual. Errors as large as this would require the transfer used be constrained to the group of transfers with an intercept velocity of 70 fps or higher.

LOS-Rate Control.- The study indicated that LOS rate could be controlled satisfactorily using a reticle, timer, and charts. This method of control, however, requires an attitude stabilized vehicle using an attitude deadband of the order of 0.3 degree. When radar LOS-rate information was used, it was possible to use the 5-degree attitude deadband during non-thrusting periods. Several runs were made using the 5-degree deadband in this manner and it was determined that approximately 5 pounds of attitude fuel could be saved for the terminal phase. For all the runs made (excluding the 5° deadband runs) the attitude fuel usage averaged about 28 pounds.

### CONCLUSIONS

This study resulted in the following conclusions:

1. A very adequate control of LOS-rate can be maintained using a reticle and timer with the LEM attitude stabilized if the GSN can be seen visually.
2. With proper LOS-rate control, the pilot can obtain a very close approximation of range and range-rate through the terminal phase of rendezvous using a range-rate time history chart for CFP transfers and a timer. This requires that an update of range, range-rate, and circularization altitude be given to the pilot by MSFN before the terminal phase begins.
3. If visual acquisition of the target and MSFN tracking are possible, the terminal phase of rendezvous can be accomplished with as much confidence and proficiency using a reticle, timer, AGS  $\Delta V$  information, AGS attitude stabilization and rendezvous charts as it can with rendezvous radar or LORS.
4. With an increase in  $\Delta V$  usage (but still within budget), the pilot can adequately control the terminal phase of rendezvous without any navigation updates even when standard deviations in range and range-rate of 10,000 feet and 16 fps exist.
5. Although a complete task analysis was not conducted, it appears from the simulations conducted that a single crew member could complete the required control tasks and chart reading with adequate residual time to maintain a minimal (emergency) timeline of radio communications and systems monitoring.

## REFERENCES

1. McDonnell Aircraft Corporation: "Gemini VI Rendezvous Procedures and Flight Charts." Gemini Design Note No. 317.
2. Moen, Gene C., Meintel, Alfred J., Kahlbaum, William M. Jr.: "A Piloted Simulation Study of the Gemini-Agena Rendezvous With and Without Canted Nozzles." Langley Working Paper No. 87.
3. Simpson, Ronald W., Stull, Paul J.: "A Study of the Dynamics Involved in GT-4 Booster Separation and Return Maneuver." MSC Internal Note No. 65-EG-41.
4. Simpson, Ronald W.: "A Hybrid Simulation Study of the GT-6 Rendezvous Maneuver." MSC Internal Note No. 65-EG-44.
5. Simpson, Ronald W., et al: "Simulation Study of Manual Control Techniques for Lunar Orbit Rendezvous," MSC Internal Note No. 65-EG-33.

## APPENDIX A

Characteristics of Simulated LEM

The LEM simulated for the purpose of this study had the following characteristics:

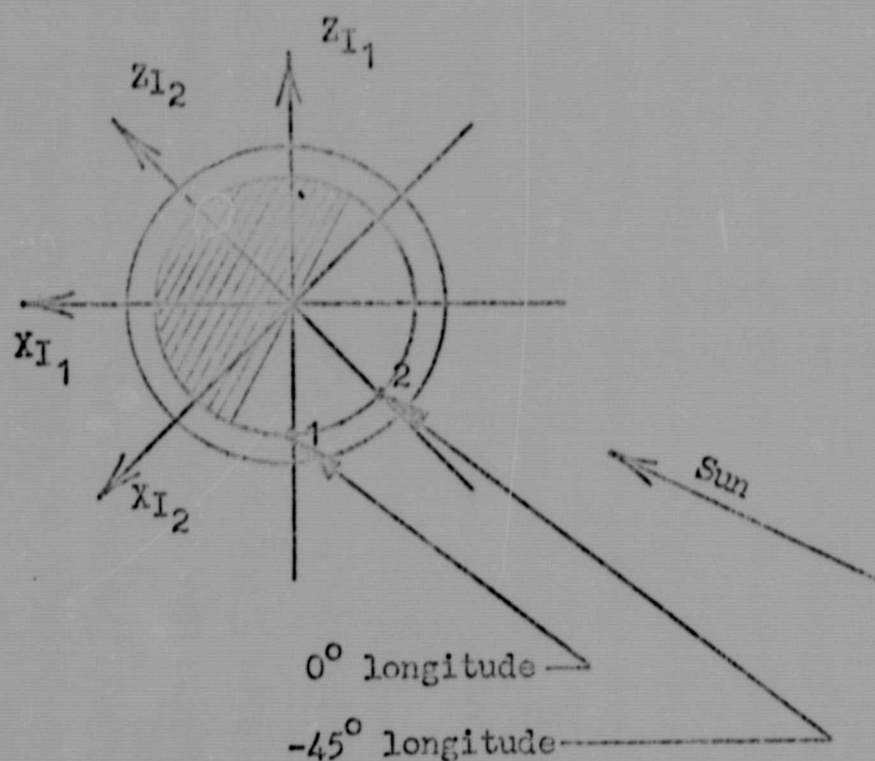
$m_o$	= 159 slugs	(initial)
$I_{xx}$	= 1476 slug ft <sup>2</sup>	(constant)
$I_{yy}$	= 2557 slug ft <sup>2</sup>	(constant)
$I_{zz}$	= 2724 slug ft <sup>2</sup>	(constant)
$I_{xy}$	= -13 slug ft <sup>2</sup>	(constant)
$I_{yz}$	= -44 slug ft <sup>2</sup>	(constant)
$I_{xz}$	= -173 slug ft <sup>2</sup>	(constant)
$\bar{X}_{cg}$	= 0.0333 ft	(constant)
$\bar{Y}_{cg}$	= 0.0500 ft	(constant)
$\bar{Z}_{cg}$	= 0.000 ft	(constant)
$Z_{pads}$	= +14.23 ft	(constant)
$Z_{RCS}$	= 0.00 ft	(constant)
$M_{cp}$	= $\pm$ 1100 ft-lbs	(roll)
$M_{cq}$	= $\pm$ 1100 ft-lbs	(pitch)
$M_{cr}$	= $\pm$ 1000 ft-lbs	(yaw)
$T_x$	= $\pm$ 200 lbs	
$T_y$	= $\pm$ 200 lbs	
$T_z$	= $\pm$ 200 lbs (4 jets can be used which will give a thrust of $\pm$ 400 lbs)	
$I_{sp}(RCS)$	= 275 sec	

## APPENDIX B

Initial Conditions for Nominal CFP Transfers \*

TRANSFER	PROBLEM VARIABLES								
	$X_I$ (feet)	$Y_I$ (feet)	$Z_I$ (feet)	$\dot{X}_I$ (fps)	$\dot{Y}_I$ (fps)	$\dot{Z}_I$ (fps)	R (feet)	$\dot{R}$ (fps)	$\lambda$ (degrees)
65 n.m. $\rightarrow$ 80 n.m. transfer ( $-45^\circ$ longitude L.S.)	-38,623	0	-34,494	+54.7	0	+41.0	54,529	-67.7	+107.2
30 n.m. $\rightarrow$ 80 n.m. transfer ( $0^\circ$ longitude L.S.)	-21,848	0	+54,005	+45.4	0	+71.5	58,257	-83.3	+52.3
118 n.m. $\rightarrow$ 80 n.m. transfer ( $-45^\circ$ longitude L.S.)	+41,737	0	-23,257	-53.1	0	+13.3	47,779	-52.9	+102.1

\* The  $Z_I$  axis always represents the landing site (L.S.) local vertical and the  $X_I$  axis points in the direction of CSM orbital motion at the L.S. The  $Y_I$  axis completes the right-handed set.



APPENDIX C  
Simulation Test Matrix

Transfer	Backup Control Mode	MSFN errors used	No. of Runs
65 n.m. to 80 n.m. transfer	Case 1 (MSFN update- R/R time history chart used.)	1 $\sigma$	15
		2 $\sigma$	5
		4.5 $\sigma$	2
	Case 2 (MSFN update- AGS display of R,R)	1 $\sigma$	3
		2 $\sigma$	2
		4.5 $\sigma$	2
	Case 3 (RR)	1 $\sigma$	3
		2 $\sigma$	2
		3 $\sigma$	2
30 n.m. to 80 n.m. transfer	Case 1	1 $\sigma$	15
		2 $\sigma$	5
		4.5 $\sigma$	2
	Case 2	1 $\sigma$	3
		2 $\sigma$	2
		4.5 $\sigma$	2
	Case 3	1 $\sigma$	3
		2 $\sigma$	2
		4.5 $\sigma$	2
118 n.m. to 80 n.m. transfer	Case 1	1 $\sigma$	15
		2 $\sigma$	5
		4.5 $\sigma$	2
	Case 2	1 $\sigma$	3
		2 $\sigma$	2
		4.5 $\sigma$	2
	Case 3	1 $\sigma$	3
		2 $\sigma$	2
		4.5 $\sigma$	2
30 n.m. to 80 n.m. transfer	Case 1 (no MSFN update- R/R time history chart used.)	Propagation of ascent errors $\sigma_{\text{range}}=10,000$ ft $\sigma_{\text{range}}=16$ fps	5

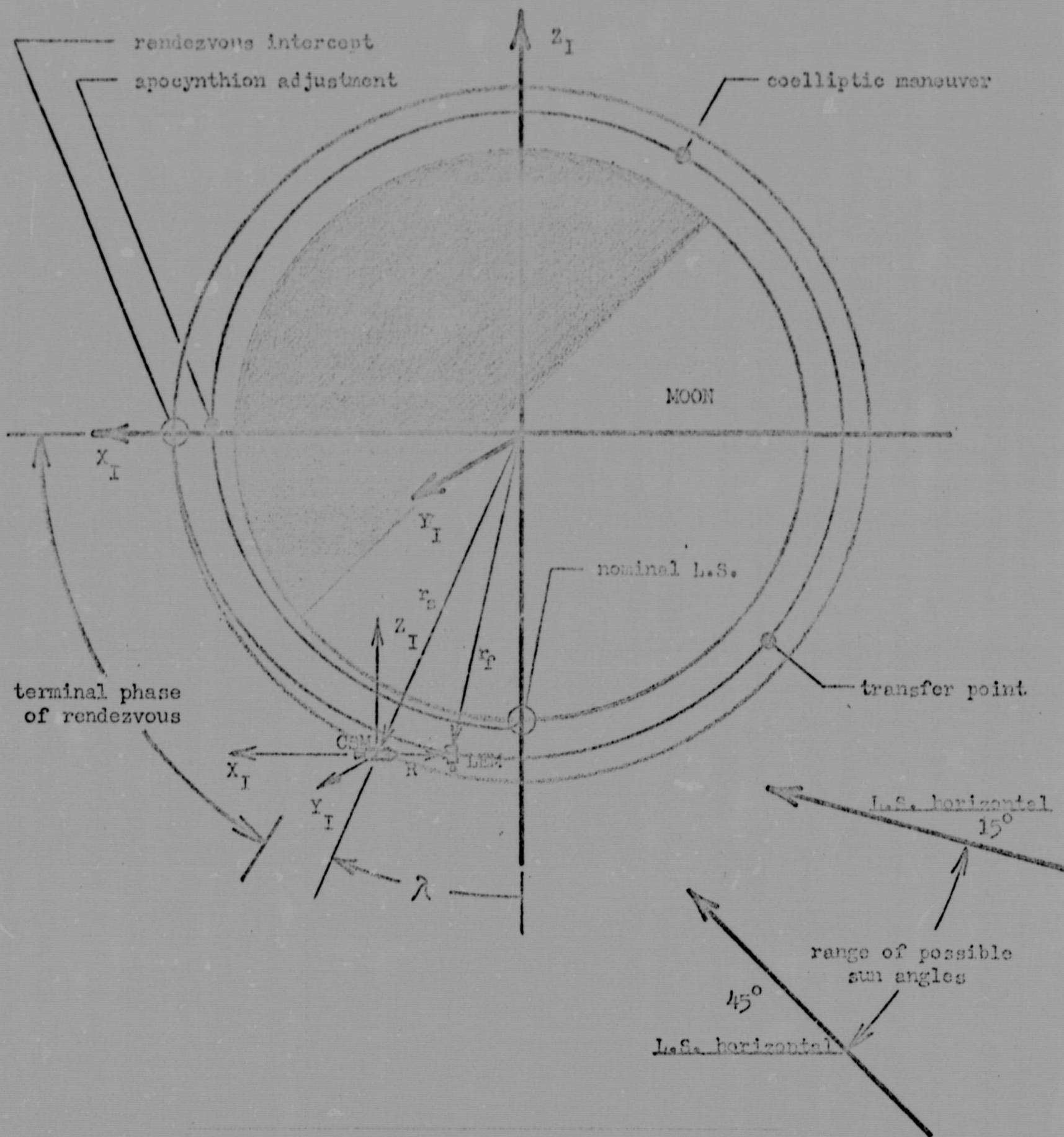


FIGURE 1 - NOMINAL CONCENTRIC FLIGHT PLAN

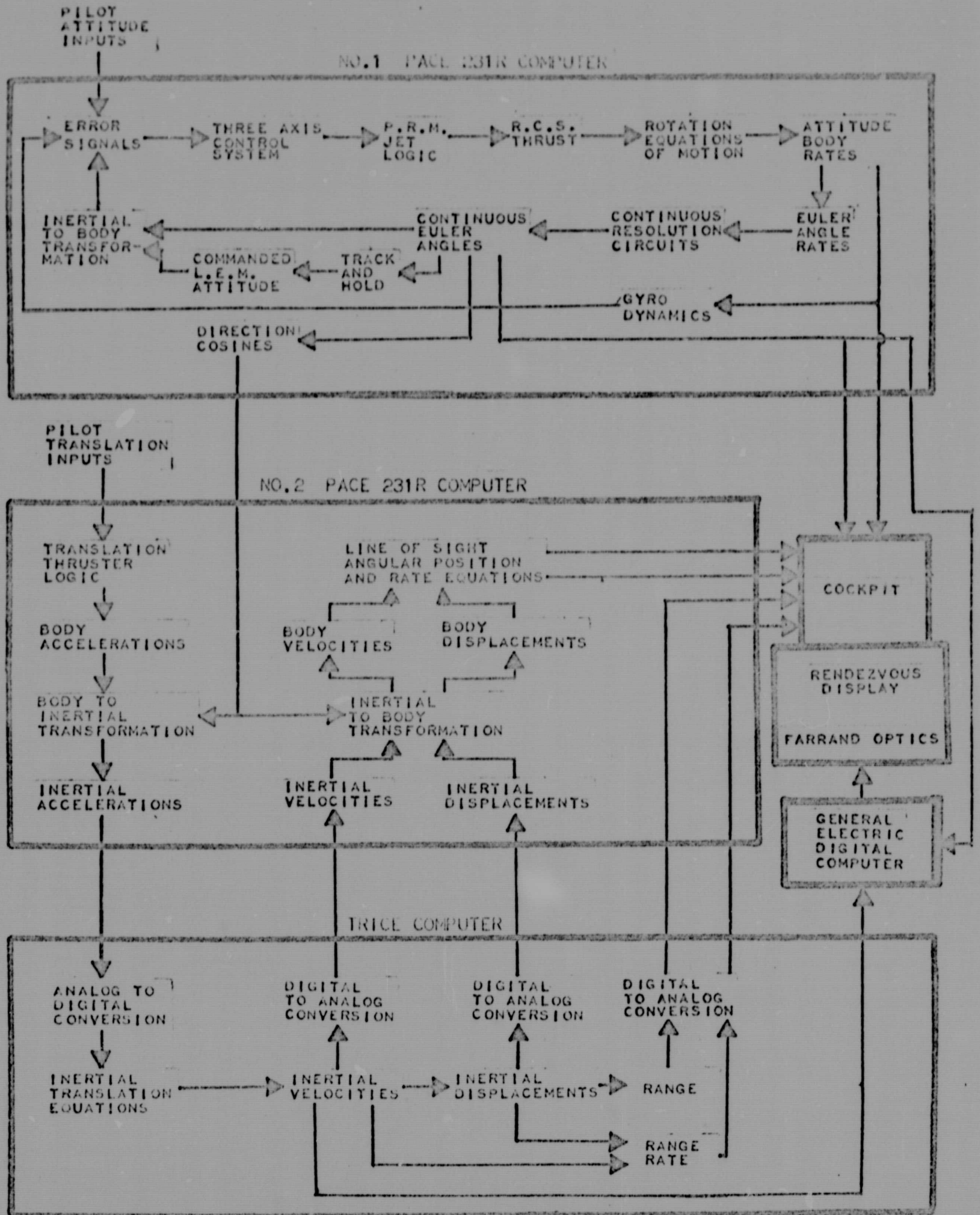


FIGURE 2 - SIMULATION BLOCK DIAGRAM

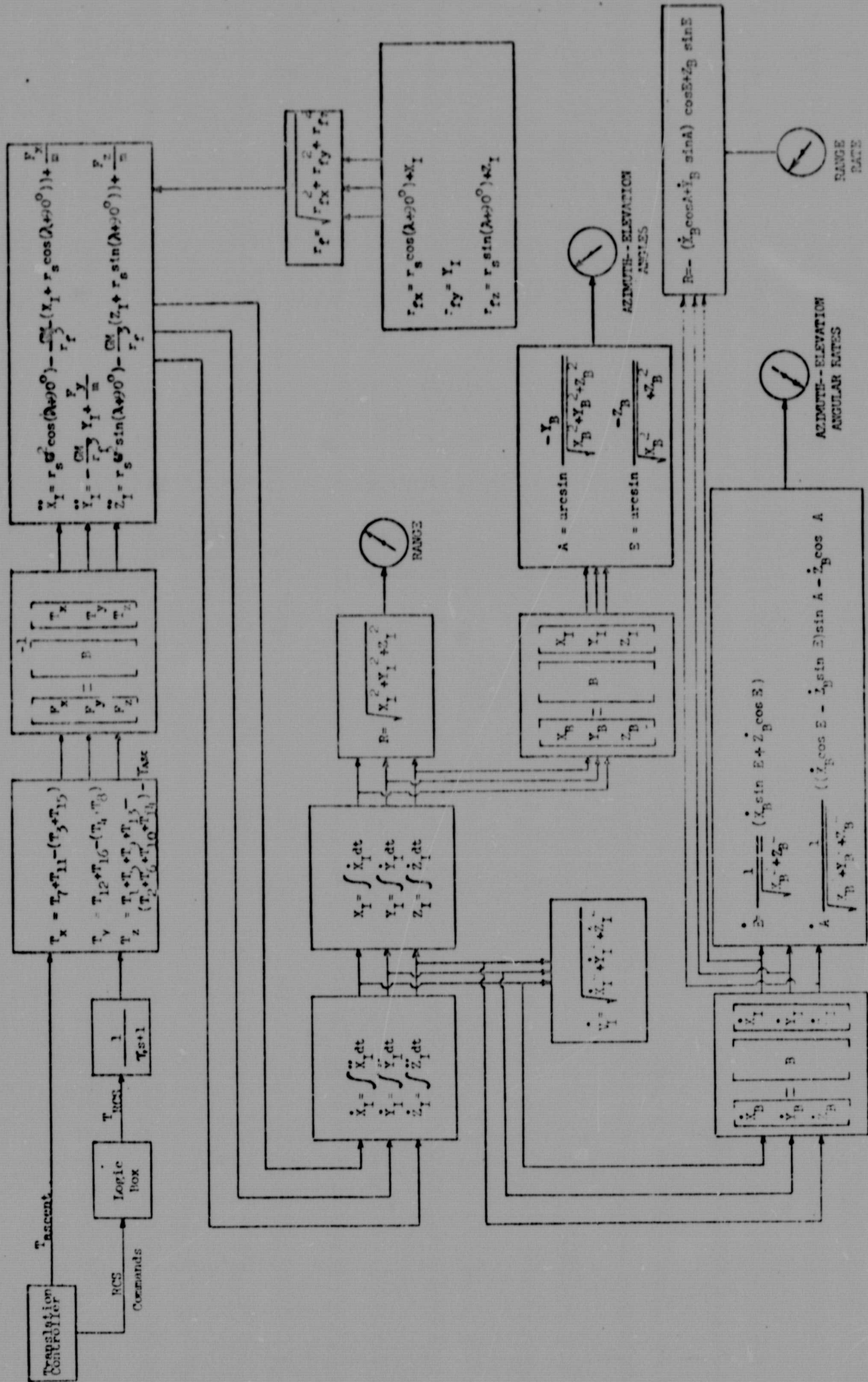
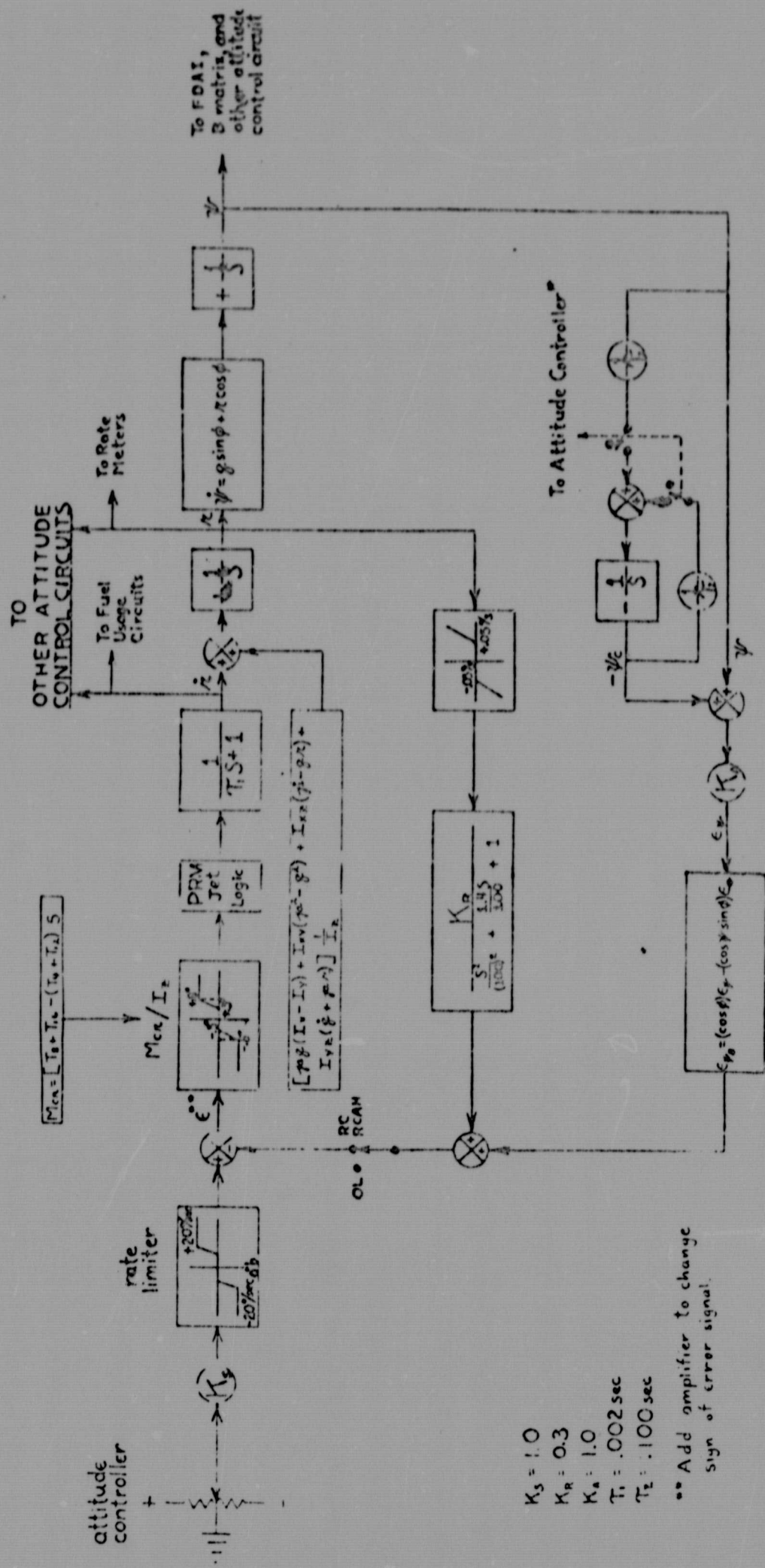


FIGURE 3 - BLOCK DIAGRAM OF TRANSLATION EQUATIONS OF MOTION





\*All switches open when stick in deadzone. When stick is out of deadzone in any axis, the followup switches in all three axes shall close.

FIGURE 5 - YAW ATTITUDE CONTROL CIRCUIT



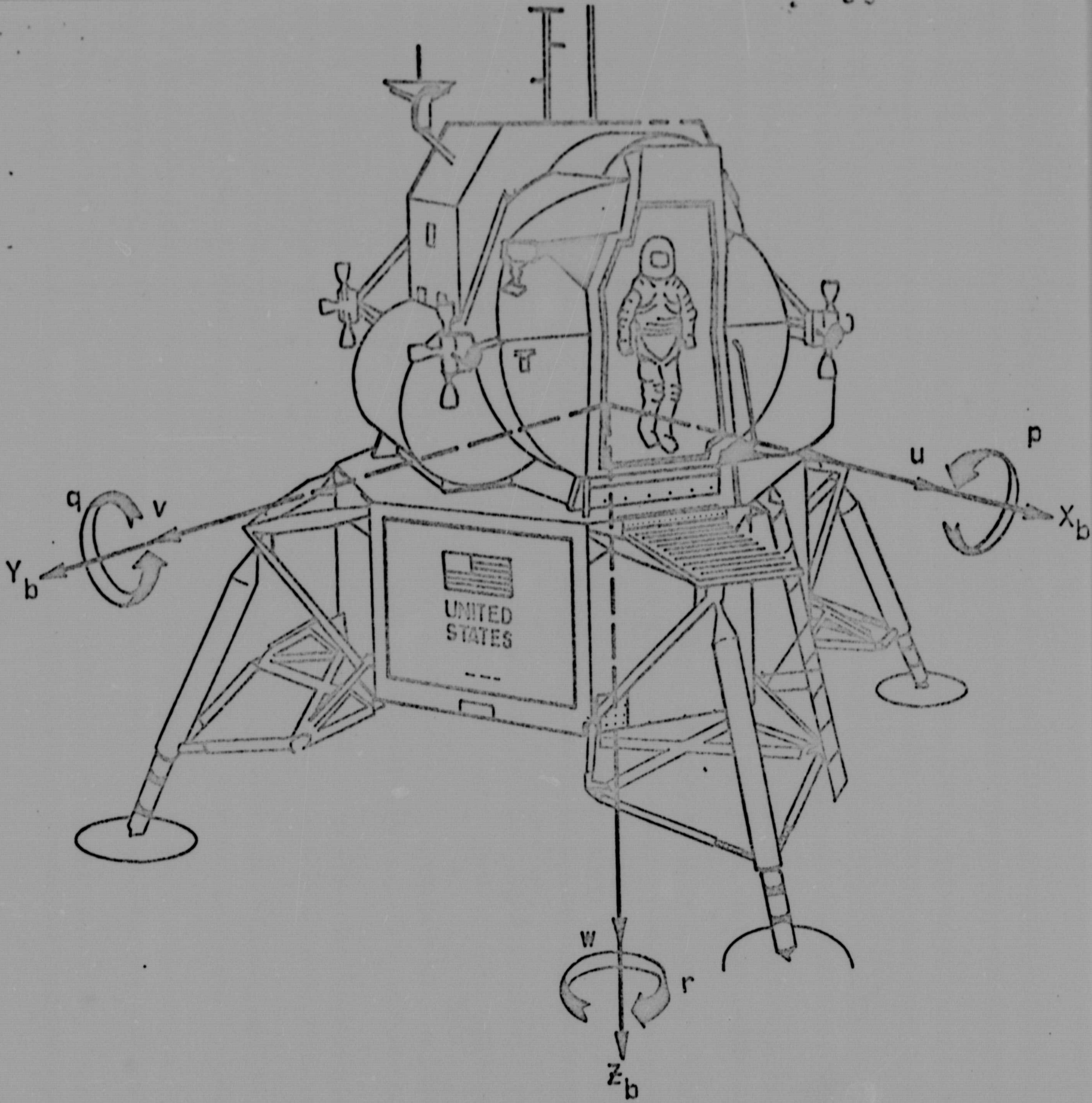


FIGURE 7 - GENERAL CONFIGURATION OF SIMULATED LEM



FIGURE 8 - SIMULATED LEM CONTROLS AND DISPLAYS

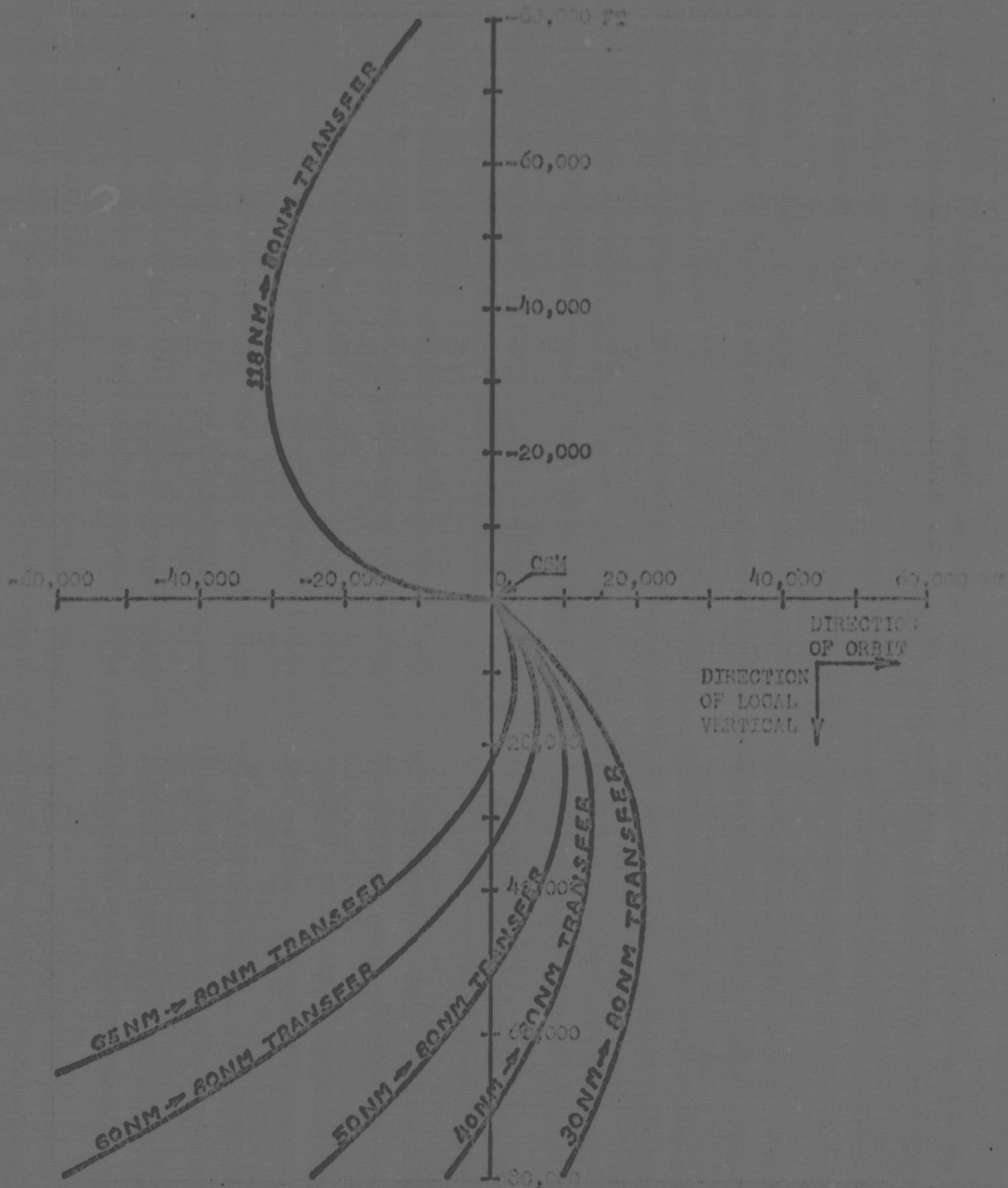


FIGURE 9 - LOCAL VERTICAL PLOT OF LEM RELATIVE POSITION FOR CFP TRANSFERS

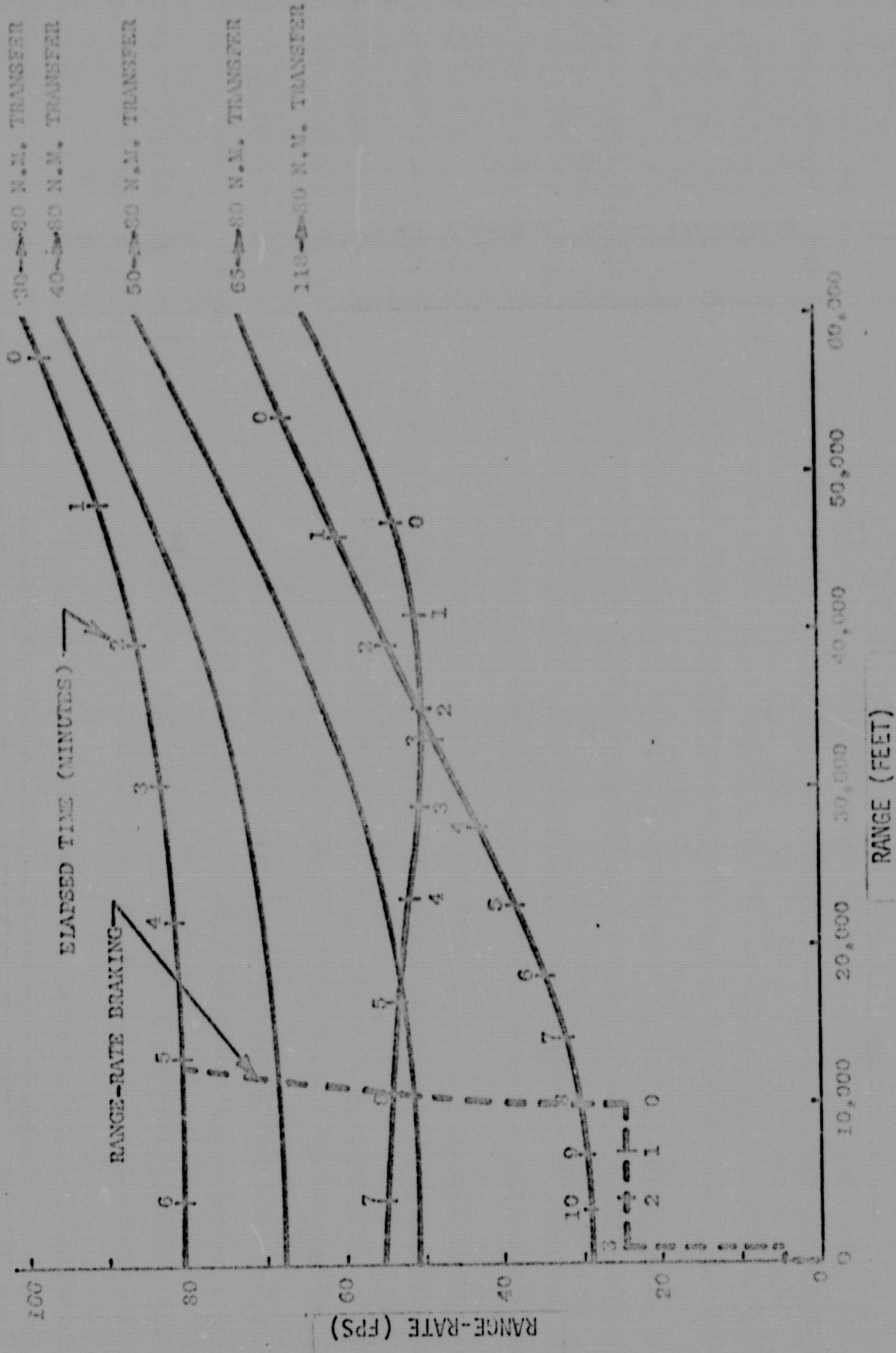


FIGURE 10 - TIME HISTORY OF RANGE-RATE VS. RANGE FOR CFP TRANSFERS

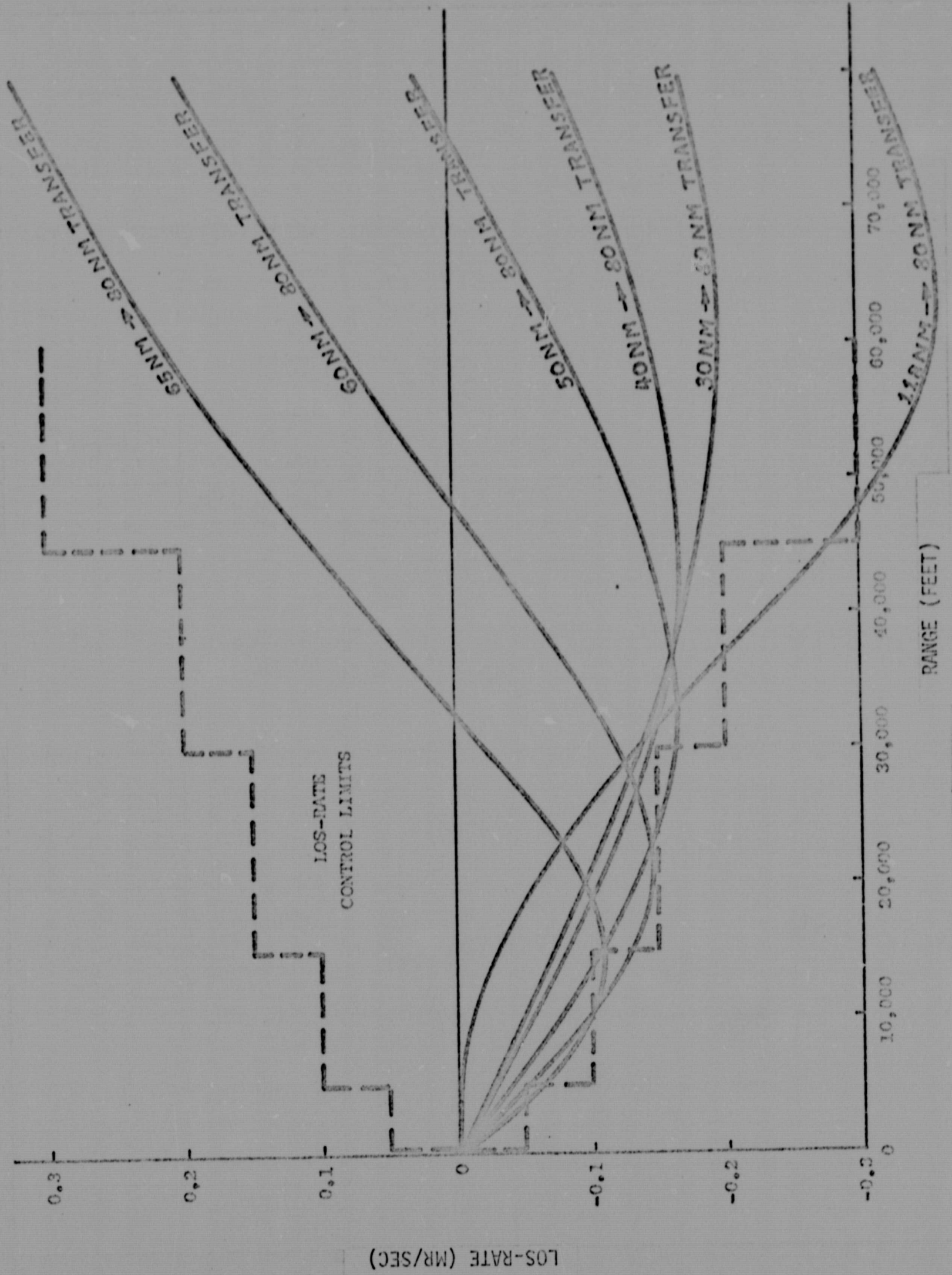


FIGURE 11 - TIME HISTORY OF LOS-RATE VS. RANGE FOR CFP TRANSFERS

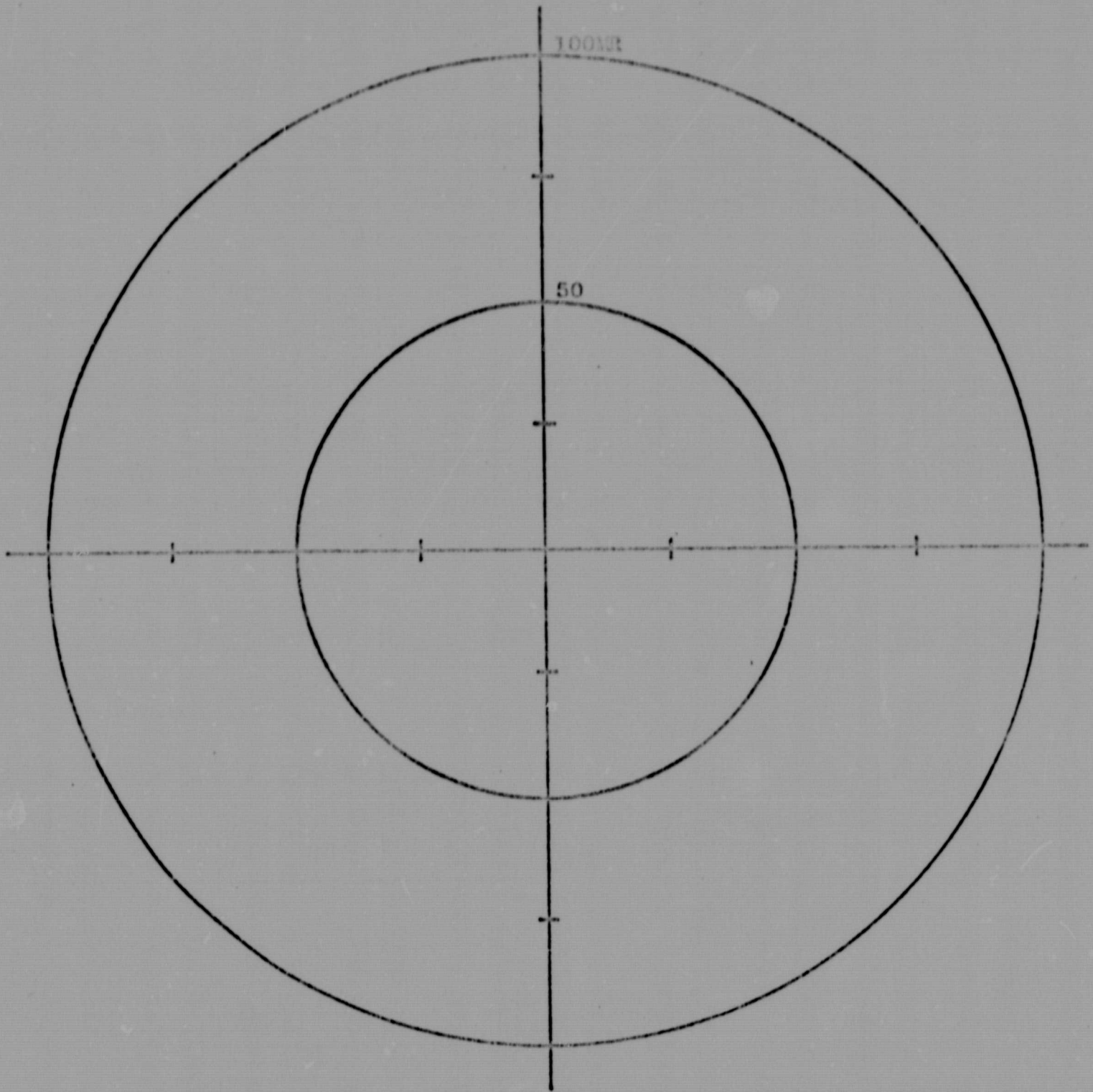


FIGURE 12 - RETICLE PATTERN

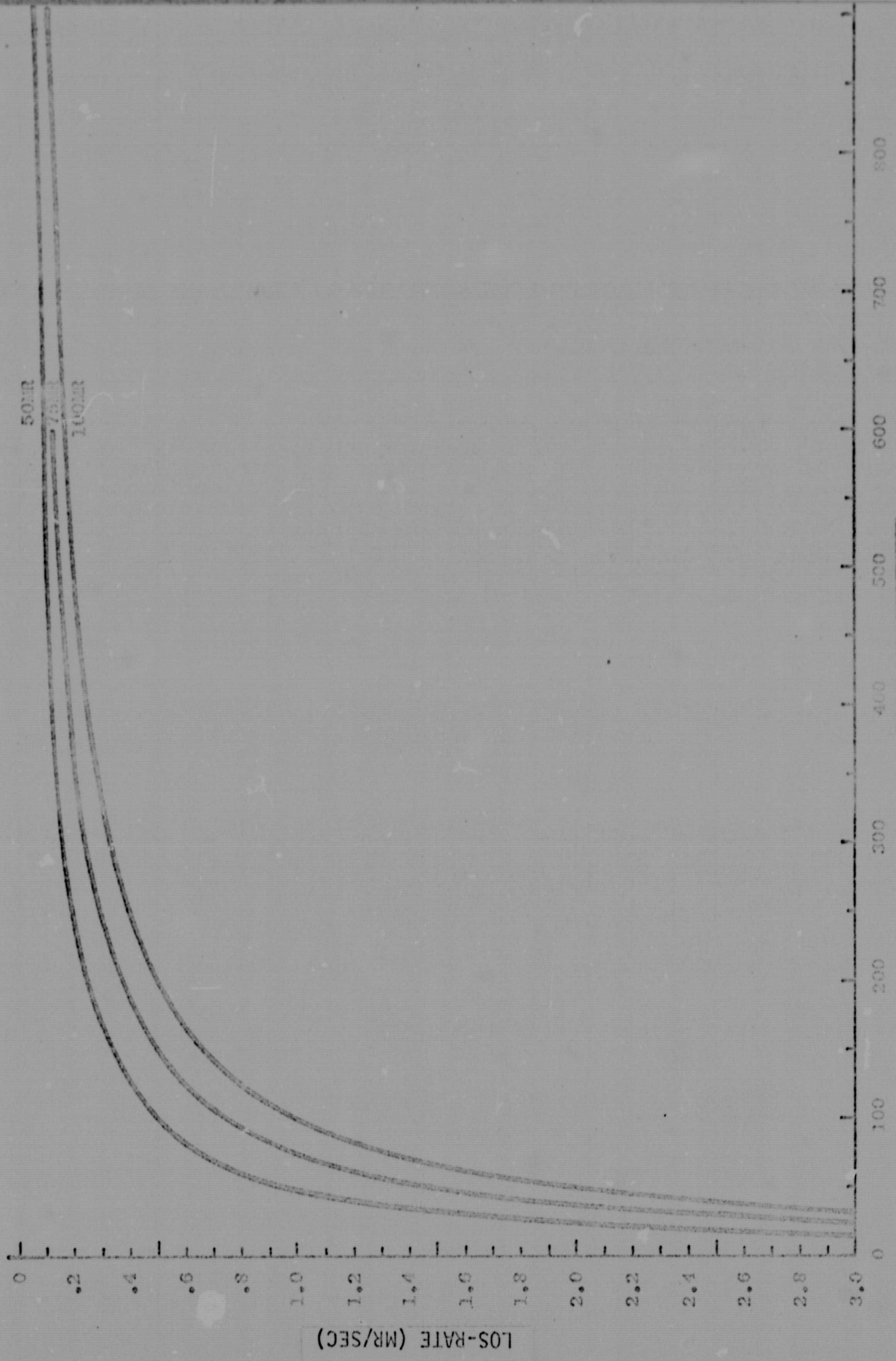


FIGURE 13 - LOS-RATE DETERMINATION USING RETICLE ELAPSED TIME

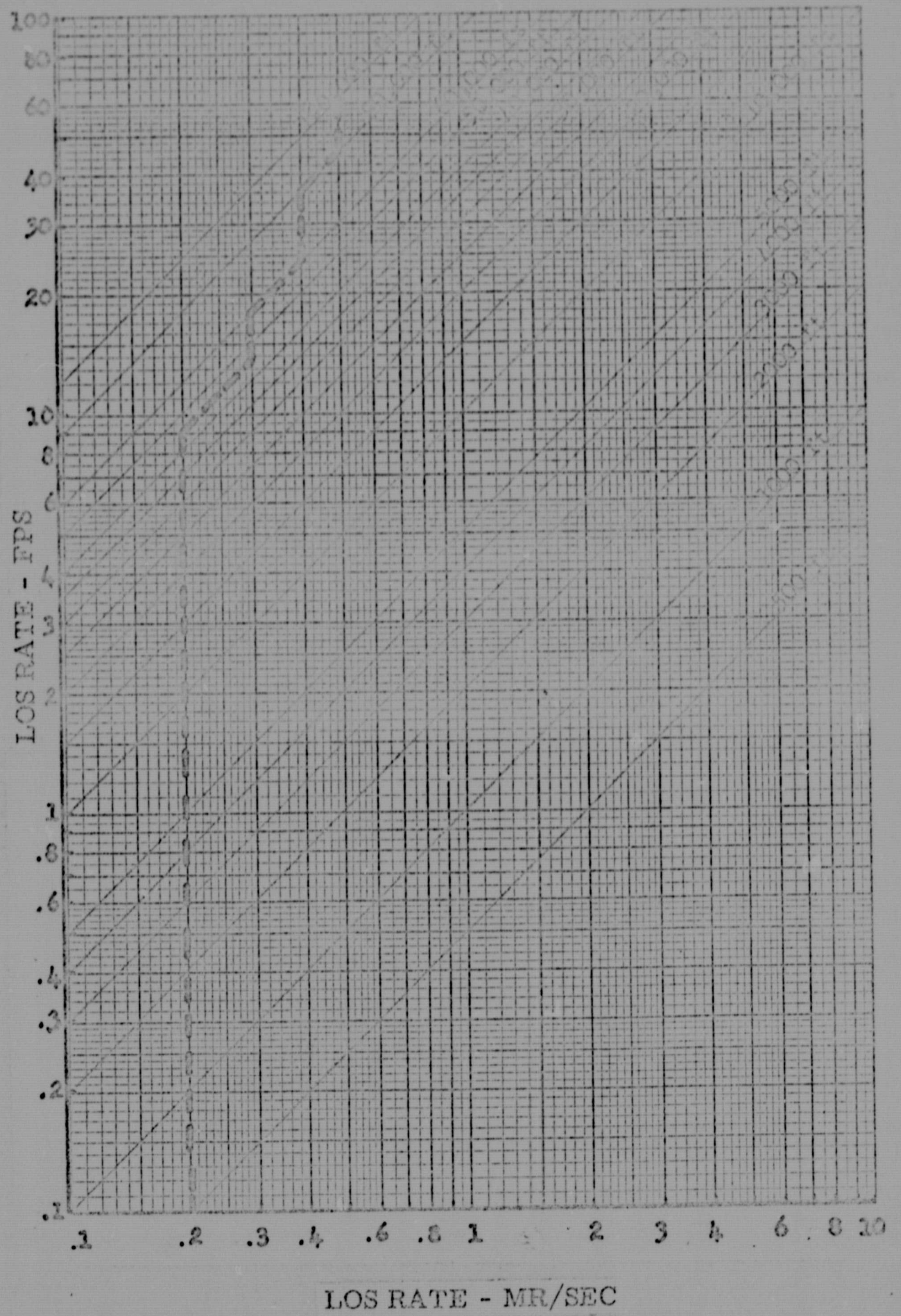
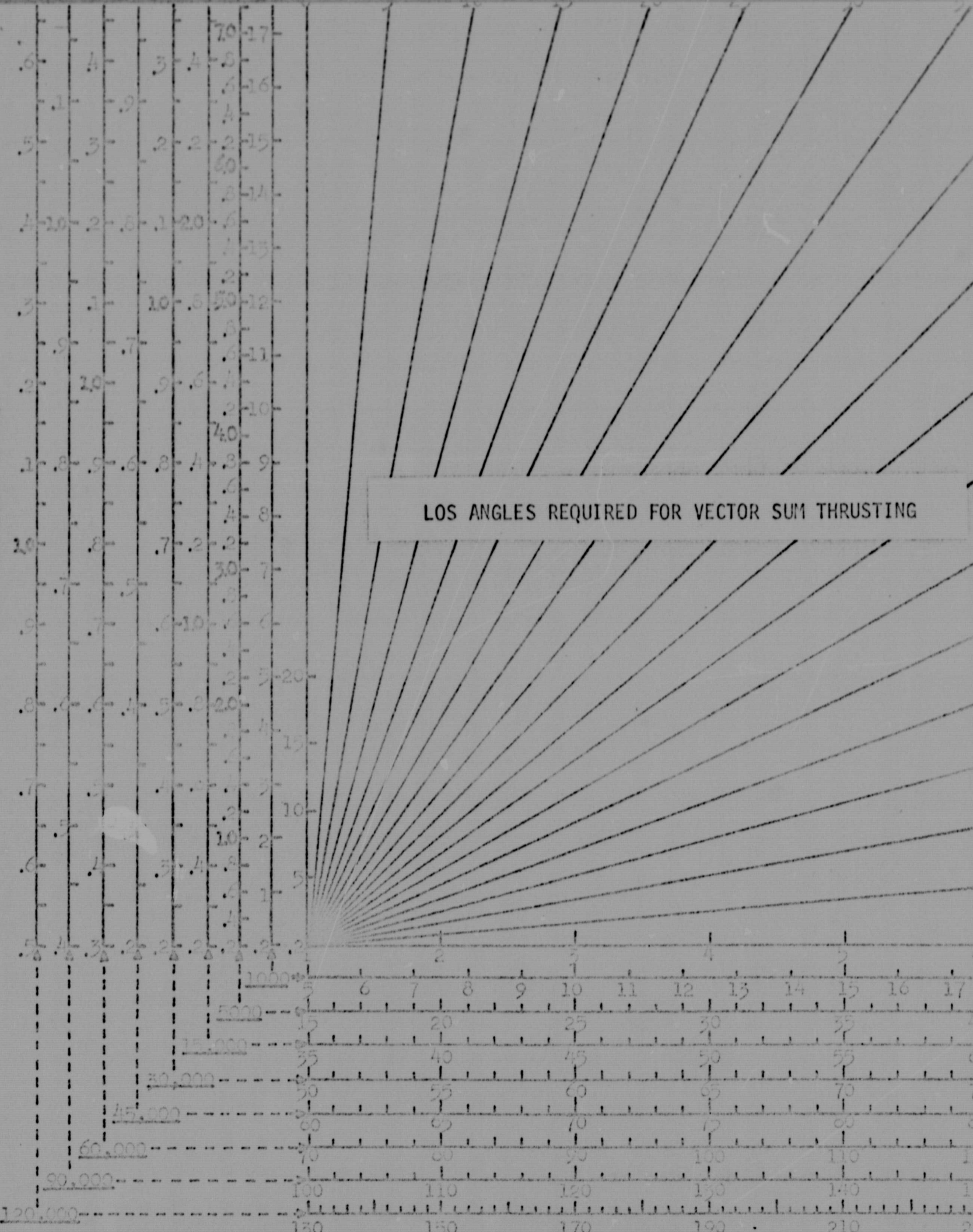


FIGURE 14 - LOS-RATE CORRECTION CHART

LOS-RATE (MR/SEC)



LOS ANGLES REQUIRED FOR VECTOR SUM THRUSTING

RANGE (FEET)

RANGE-RATE (FPS)

FIGURE 15 - RANGE-RATE/LOS-RATE VECTOR SUM CHART

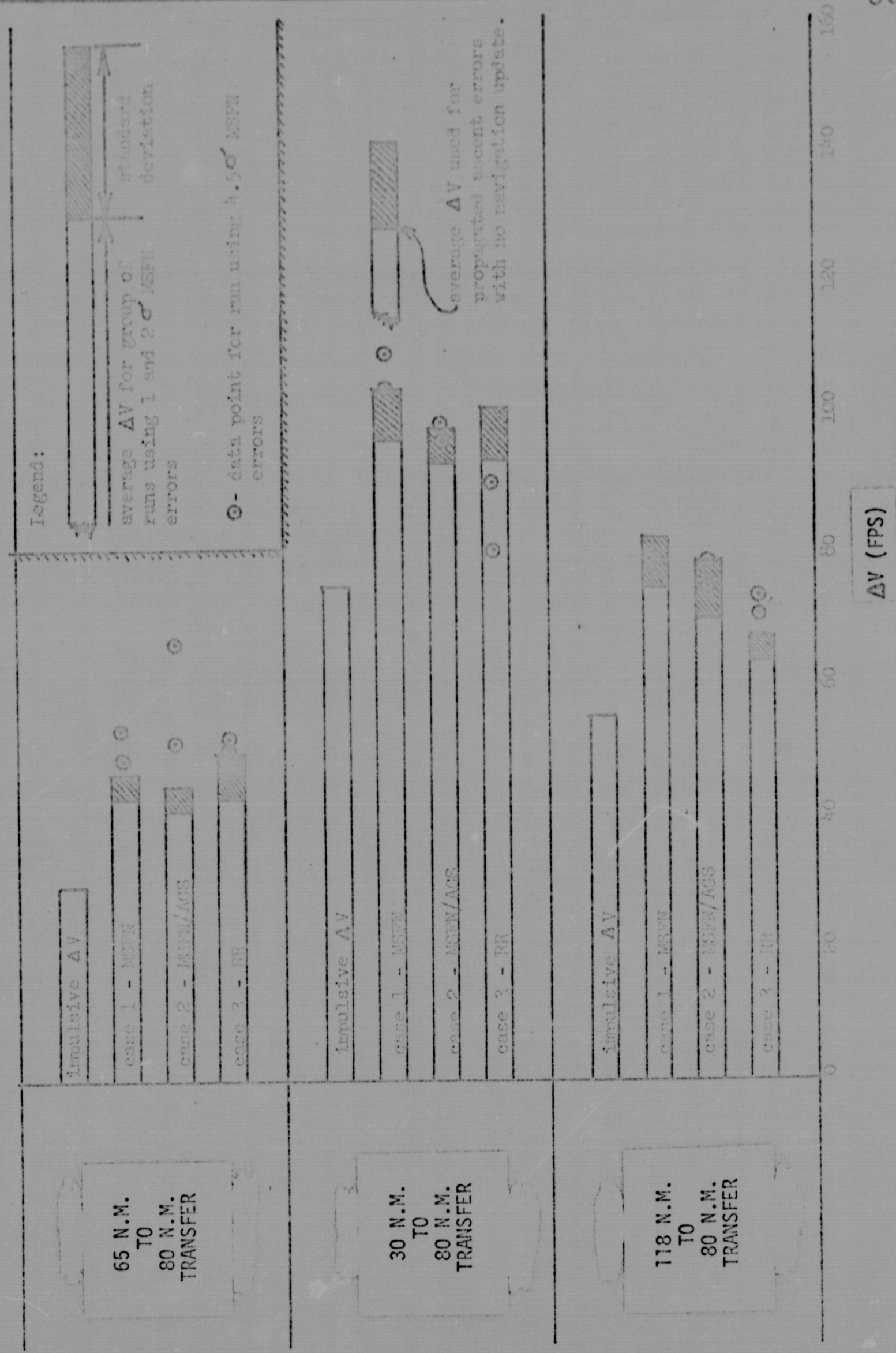


FIGURE 16 - SUMMARY OF  $\Delta V$  PERFORMANCE OF BACKUP CONTROL MODES